Calculation of dynamic responses of railway sleepers on a nonlinear foundation

Le-Hung Tran, Tien Hoang, Gilles Foret, Denis Duhamel, Dinh-Duc Nguyen

Nonlinear Dynamics manuscript No.
(will be inserted by the editor)

Calculation of dynamic responses of railway sleepers on a nonlinear foundation

Le-Hung Tran · Tien Hoang · Gilles Foret · Denis Duhamel · Dinh-Duc Nguyen

Received: date / Accepted: date

Abstract The safety of a passing train depends on different factors, of which one of the most important is the behavior of the foundation. Therefore, the effects of the non-linearity of ballast on the dynamic responses of the railway track are a key research interest. In this paper, a new model of railway sleepers posed on a nonlinear foundation has been developed. By coupling the finite element method (FEM) of the sleeper with an analytical model of the periodically supported beam model, the dynamic equation of the sleeper is developed. On the other hand, by considering a periodic series of moving loads, this equation can be transformed to a forced nonlinear oscillation. Iteration procedures have been built to calculate the periodic solution. This method has demonstrated a good convergence of results by comparison with the analytical solution in the linear case. The influence of the nonlinear foundation has been investigated by two examples: cubic-nonlinear and bi-linear foundations. The parametric studies demonstrate that numerical results converge with a small number of iterations.

Keywords Railway track · railway sleeper · nonlinear foundation · harmonic balance · structural dynamic

Le Hung Tran
Faculty of Civil Engineering - VNU Hanoi, University of Engineering and Technology, 144 Xuan Thuy Street, Cau Giay District, Hanoi, Vietnam
E-mail: hungtl@vnu.edu.vn

Tien Hoang, Gilles Foret, Denis Duhamel
Laboratoire Navier, UMR 8205, Ecole des Ponts, Université Gustave Eiffel, CNRS, Champs-sur-Marne, 77455 Marne-la-Vallée Cedex 2, France

Dinh-Duc Nguyen
Factulty of Civil Engineering - VNU Hanoi, University of Engineering and Technology, 144 Xuan Thuy Street, Cau Giay District, Hanoi, Vietnam

1 Introduction

The stability of the railway track is one of the research interests of railway engineers as it is key to the safety of the passing trains. Consequently, many research projects have been undertaken to analyze the dynamic responses of the railway track subjected to moving loads. Firstly, analytical models have been developed for an infinite beam placed on a continuous foundation. Krylov [1] and Timoshenko [2] are the pioneering researchers in this domain, in which the dynamic stresses are calculated for simply supported beams under moving loads. By using the same method, Fryba [3] studied the transverse vibrations of a beam posed on an elastic foundation, in which the beam responses are calculated by the sum of multiple normal modes. The free vibrations of the beam on an elastic foundation has been solved analytically by Timoshenko et al. [4]. Analytical and numerical methods have been developed for various foundations such as: Winkler, Pasternak, Vlasov or Reissner [5–12]. In order to take into account the distribution of discrete supports, Mead [13,14] developed the periodically supported beam model under moving loads for the rail. This model type has been also investigated for elastic foundations [15–18]. A fast analytical method to calculate the dynamic responses of railway sleepers has been presented by Tran et al. [19, 20]. Most recently, in order to study the influence of non homogeneous foundation on the sleeper responses, Tran et al. [21] developed a semi-analytical model by coupling a numerical model for the sleeper and a periodically supported beam model for the rail.

The two models which are frequently used to describe the nonlinear behaviors of foundation are cubic-nonlinear and bi-linear foundations. The cubic law describes a foundation reaction which has a cubic dependence on displacement. The bi-linear foundation presents a foundation behavior which has two different linear behaviors: one in compression and one in tension. By taking into account the non-linearity of the foundation on the model of the beam placed on a continuous foundation, the solutions have been calculated by using different techniques. Ding et al. [22,23] solved the problem with the help of the Galerkin discretization and a fourth-order Runge-Kutta method. Abdelghany et al. [24], Kargarnovin et al. [25] and Ansari et al. [26] used the same method to calculate the responses of the beam under a harmonic load or to calculate the resonance of the beam. Chen et al. [27, 28] studied the convergence of Galerkin truncation for the sandwich beam on a nonlinear foundation and a scheme to determine the convergence of this model has been presented. Recently, Ouzizi et al. [29] presented a model of the dynamic responses of the beam on a nonlinear frictional viscoelastic foundation with the help of an explicit scheme. The dynamic track responses are computed by using the finite element method [30–32]. A numerical method has been also developed to calculate the solutions of the beam in the case of tensionless foundation [33–35]. The nonlinear responses of beams subjected to moving loads carrying multiple mass-spring-damper attachments has been also studied [36–41]. However, the effect of the non-linearity of the foundation is not easy to take into account in the periodically supported beam model.

In this paper, we present a novel model to calculate the solution of dynamic behavior of a railway sleeper posed on a nonlinear foundation. In Section 2, the dynamic equation of the sleeper is written with the help of a finite element model. When the rails are modeled as a periodically supported beam [42,43], a relation between the rail displacements and the reaction force in the frequency domain can be obtained and it holds for any foundation behavior. Therefore, the forces applied by the rails on the sleeper can be rewritten in the dynamic equation of the sleepers with the help of the Dirac delta function. By considering that the moving loads are a periodic series, this equation is equivalent to a forced nonlinear oscillator. Then, a numerical method is developed with the help of the harmonic balance method and the iteration procedures for nonlinear oscillators [44, 45] in Section 3. The numerical applications are shown in Section 4. In the linear case, the numerical results converge to the analytical solutions [46]. Thereafter, the dynamic responses of the sleepers are calculated for two types of nonlinear foundation: cubic law and bi-linear foundation. The applications show that the numerical results converge rapidly to the solution of the problem. In addition, parametric studies have been conducted to analyze the influence of nonlinear parameters on the sleeper responses. Finally, conclusions are drawn in Section 5.

2 Formulations

Let us consider the railway track shown in Fig. 1. In this track, the rails k (with $k = [1, 2]$) are subjected to moving loads $Q_j^{(k)}$ which are characterized by the distance to the first wheel D_j ($1 \leq j \leq K$ where K is the total number of axles). The mutual distance D_j of the moving loads is not restricted to be constant. The rails are periodically supported by the sleepers and each one is separated by a length l. Next, a novel dynamic model of the sleeper is developed by taking into account the non-linearity of the foundation.

2.1 Sleeper posed on a foundation

Fig. 2 presents a finite element model of the sleeper posed on a non linear foundation. In this model, we use the beam element in 2D where each node has 3 degrees of freedom (DOFs) which correspond to the 2 displacements (u_x, u_z) and 1 rotation (θ_y). The sleeper is subjected to vertical forces at two nodes: R_1 and R_2 which are the two rail positions. If n_n is the number of nodes, the number of DOFs is $3n_n$. We note that the main dynamic response of the system is in the vertical direction. Each node of the sleeper is related with the foundation by a nonlinear system which describes the behavior of the foundation in two parts: linear and nonlinear. The linear term is modelled by a stiffness k_f and damping coefficients ζ_f. Meanwhile the nonlinear term of the foundation is written in the function $\mathbf{f}_{NL}(\mathbf{u}, \dot{\mathbf{u}})$.

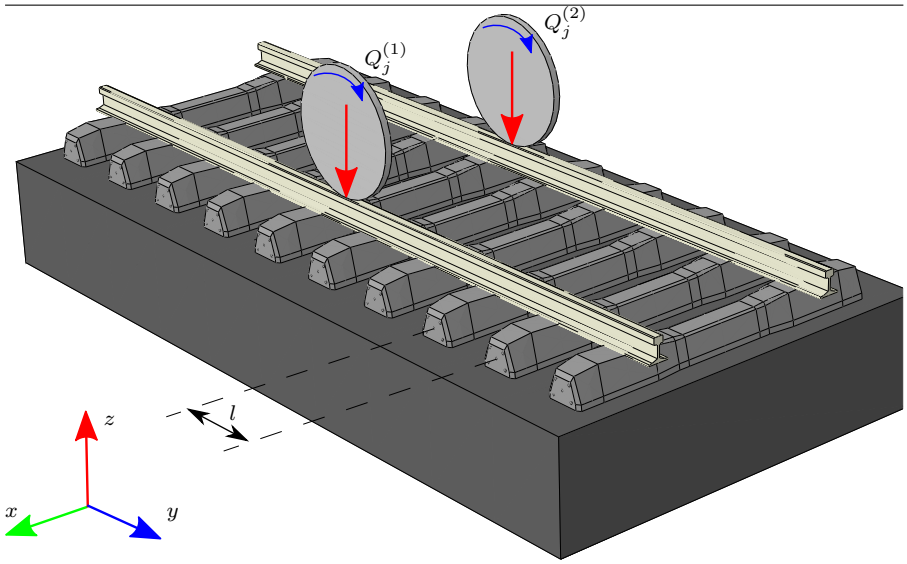

Fig. 1: Ballasted railway track

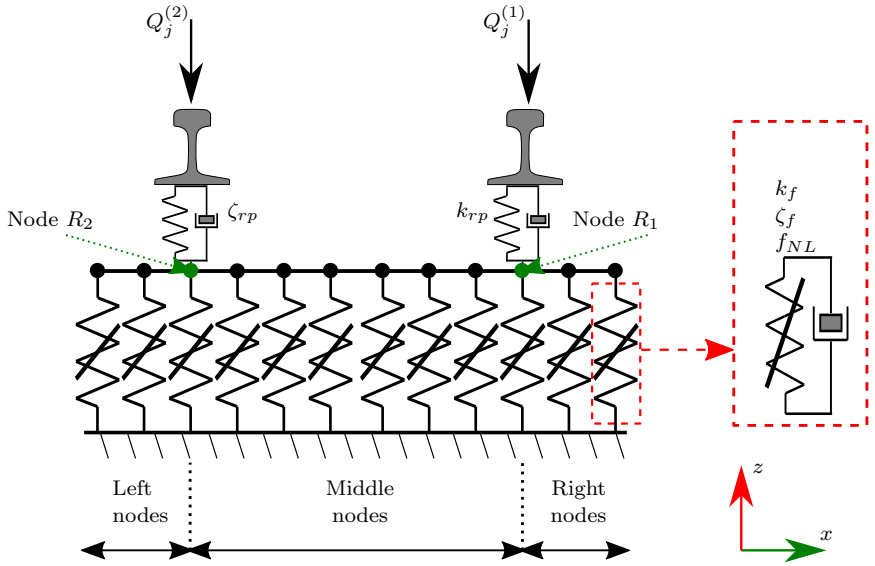

Fig. 2: Finite element model of the railway sleeper posed on a nonlinear foundation and subjected to the moving loads

The dynamic equation of the sleeper posed on a foundation is obtained by using a finite element method as follows:

$$\mathbf{M}_s\ddot{\mathbf{u}} + \mathbf{K}_s\mathbf{u} + \mathbf{F}_f(\mathbf{u}) = \mathbf{F}_R(t) \tag{1}$$

where $\mathbf{M}_s$ and $\mathbf{K}_s$ represent respectively the mass and rigidity matrices of the sleeper which are generated with the help of FEM where the notation $\left(\dot{\square}\right)$ denotes the partial derivative with respect to time t. $\mathbf{u}$ is a vector of nodal displacements of sleepers and:

$$\mathbf{u}_i = \mathbf{u}(x_i) = [u_x(x_i), u_z(x_i), \theta_z(x_i)]^T$$

for the i^{th} node of a sleeper. The vector $\mathbf{F}_R(t)$ describes a force applied on the sleeper for the two rail positions (see Fig. 2). The vector $\mathbf{F}_f(\mathbf{u})$ represents the force induced by the foundation on the sleeper and we suppose that this force follows only the vertical direction. For this reason, $\mathbf{F}_f(\mathbf{u})$ can be calculated as follows:

$$\mathbf{F}_f(\mathbf{u}) = k_f \mathbf{I}_{u_z} \mathbf{u} + \zeta_f \mathbf{I}_{u_z} \dot{\mathbf{u}} + \mathbf{I}_{u_z} \mathbf{f}_{NL}(\mathbf{u}, \dot{\mathbf{u}}) \tag{2}$$

The matrix $\mathbf{I}_{u_z}$ is calculated as follows:

$$\mathbf{I}_{u_z} = \mathbf{e}_{u_z} \otimes \mathbf{e}_{u_z}$$

where the symbol $\otimes$ denotes the tensor product. The vector $\mathbf{e}_{u_z}$ which has $3n_n$ components is defined as follows:

$$\mathbf{e}_{u_z} = \left[0\ 1\ 0\ 0\ 1\ 0 \cdots 0\ 1\ 0\right]^T$$

2.2 Rail pad

A rail pad which is located between the rails and the sleeper, can be modeled as a spring-damper system with stiffness k_{rp} and damping coefficient ζ_{rp}. The reaction force of the sleeper to the rail k is expressed as follows:

$$R_k(t) = -\zeta_{rp}\left[\dot{w}_r^{(k)}(t) - \dot{u}_{R_{kz}}(t)\right] - k_{rp}\left[w_r^{(k)}(t) - u_{R_{kz}}(t)\right] \tag{3}$$

where $w_r^{(k)}(t)$ and $u_{R_{kz}}(t)$ are respectively the rail and sleeper vertical displacement at the contact positions between the rail k and sleeper in time domain. So that, we can deduce the expression of the reaction force applied vertically on the beam at two rail positions:

$$\mathbf{F}_R(t) = -R_1(t)\mathbf{e}_{R_1} - R_2(t)\mathbf{e}_{R_2} \tag{4}$$

The vectors $\mathbf{e}_{R_1}$, $\mathbf{e}_{R_2}$ are two column vectors which each have $3n_n$ elements. The two vectors are zero everywhere, except at the positions which correspond to the vertical displacement of the two nodes R_1 and R_2 where they have the value 1.

Moreover, by using the Fourier transform, Eq. (3) can be rewritten in the frequency domain:

$$\hat{R}_k(\omega) = -k_p\left[\hat{w}_r^{(k)}(\omega) - \hat{u}_{R_{kz}}(\omega)\right] \tag{5}$$

where $k_p = k_{rp} + \mathrm{i}\omega\zeta_{rp}$ is the dynamic stiffness of the rail pad, ω is the angular velocity and $\mathrm{i}^2 = -1$. $\hat{w}_r^{(k)}$ and $\hat{u}_{R_{kz}}$ are respectively the rail k and sleeper vertical displacements at the crossing point in the frequency domain. By inserting Eq. (23) into Eq. (5) (see B), we obtain the following results:

$$\begin{cases} \hat{w}_r^{(k)}(\omega) = \dfrac{k_p \hat{u}_{R_{kz}}(\omega) - \mathcal{Q}_k}{k_p + \mathcal{K}_e} \\ \hat{R}_k(\omega) = \dfrac{k_p}{k_p + \mathcal{K}_e} \left[\mathcal{K}_e \hat{u}_{R_{kz}}(\omega) + \mathcal{Q}_k\right] \end{cases} \tag{6}$$

2.3 Dynamic equation of the railway sleeper

By substituting Eqs. (2) and (4) into Eq. (1), the dynamic equation of the sleeper under a moving load and resting on the nonlinear foundation can be written as follows:

$$\begin{aligned} \mathbf{M}\ddot{\mathbf{u}} + \mathbf{C}\dot{\mathbf{u}} + \mathbf{K}\mathbf{u} + \mathbf{f}_{NL}(\mathbf{u}, \dot{\mathbf{u}}) = &\left[k_{rp} w_r^{(1)}(t) + \zeta_{rp} \dot{w}_r^{(1)}(t)\right] \mathbf{e}_{R_1} \\ &+ \left[k_{rp} w_r^{(2)}(t) + \zeta_{rp} \dot{w}_r^{(2)}(t)\right] \mathbf{e}_{R_2} \end{aligned} \tag{7}$$

where $w_r^{(1)}(t)$ and $w_r^{(2)}(t)$ denote respectively the displacements of the rails 1 and 2 at the two contact points with the sleeper. $\mathbf{M}$, $\mathbf{C}$, $\mathbf{K}$ are the mass, damping and rigidity matrices, which represent the linear part of the model. Beside, the term $\mathbf{f}_{NL}(\mathbf{u}, \dot{\mathbf{u}})$ is a vector that describes the non-linear behavior of the model. These matrices are calculated as follows:

$$\begin{cases} \mathbf{K} = \mathbf{K}_s + k_f \mathbf{I}_{u_z} + k_{rp} \mathbf{I}_{R_1} + k_{rp} \mathbf{I}_{R_2} \\ \mathbf{C} = \zeta_f \mathbf{I}_{u_z} + \zeta_{rp} \mathbf{I}_{R_1} + \zeta_{rp} \mathbf{I}_{R_2} \\ \mathbf{M} = \mathbf{M}_s \end{cases}$$

where matrix $\mathbf{I}_{R_1}$ is the null matrix with size $3n_n \times 3n_n$, except the component which corresponds to the position (R_1, R_1) get the value 1, same for matrix $\mathbf{I}_{R_2}$. In other word, the two matrices are calculated by:

$$\begin{cases} \mathbf{I}_{R_1} = \mathbf{e}_{R_1} \otimes \mathbf{e}_{R_1} \\ \mathbf{I}_{R_2} = \mathbf{e}_{R_2} \otimes \mathbf{e}_{R_2} \end{cases}$$

The right side of Eq. (7) depends on the rail displacement. By substituting Eq. (6) into Eq. (7), the dynamic equation of the railway sleeper can be rewritten

as a function of the sleeper displacement as follows (see A):

$$\begin{aligned}\mathbf{M}\ddot{\mathbf{u}} + \mathbf{C}\dot{\mathbf{u}} + \mathbf{K}\mathbf{u} + \mathbf{f}_{NL}(\mathbf{u}, \dot{\mathbf{u}}) = \mathbf{I}_R &\left[\frac{1}{2\pi}\int_{-\infty}^{+\infty} \frac{k_p^2 \hat{\mathbf{u}}(\omega)}{k_p + \mathcal{K}_e} \mathrm{e}^{\mathrm{i}\omega t}\mathrm{d}\omega\right] \\ &- \left[\frac{1}{2\pi}\int_{-\infty}^{+\infty} \frac{k_p \mathcal{Q}_1(\omega)}{k_p + \mathcal{K}_e} \mathrm{e}^{\mathrm{i}\omega t}\mathrm{d}\omega\right] \mathbf{e}_{R_1} \\ &- \left[\frac{1}{2\pi}\int_{-\infty}^{+\infty} \frac{k_p \mathcal{Q}_2(\omega)}{k_p + \mathcal{K}_e} \mathrm{e}^{\mathrm{i}\omega t}\mathrm{d}\omega\right] \mathbf{e}_{R_2}\end{aligned} \tag{8}$$

where $\mathbf{I}_R = \mathbf{I}_{R_1} + \mathbf{I}_{R_2}$. This equation describes the dynamic responses of the railway sleeper posed on the nonlinear foundation and it is similar to that of a nonlinear oscillator. The right side of the equation represents the interaction between the rails and the sleeper at the two rail positions. In next step, in order to simplify these terms, we consider only periodic solutions when the moving forces are a periodic series.

2.4 Periodic series of moving loads

We consider that the train contains many identical wagons as shown in Fig. 3). The distances D_j of each wheel are characterized by:

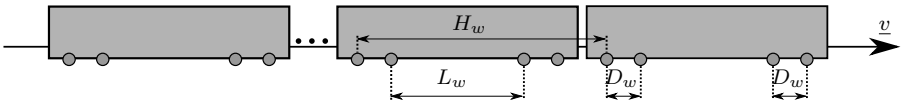

Fig. 3: Diagram of the periodic series of moving loads

$$D_j = \begin{cases} jH_w & \text{for wheel 1 of wagon} \\ jH_w + D_w & \text{for wheel 2 of wagon} \\ jH_w + D_w + L_w & \text{for wheel 3 of wagon} \\ jH_w + 2D_w + L_w & \text{for wheel 4 of wagon} \end{cases} \tag{9}$$

where D_w is the distance of the bogie, H_w is the length of the wagon and L_w is the distance between wheels 2 and 3 of a wagon (see Fig. 3). This series of moving loads may be used to represent the series of charges for a railway track. In addition, we consider that the loads $Q_j^{(k)}$ of each wheel j on each rail k are equal:

$$Q_j^{(k)} = Q \tag{10}$$

By considering infinite periodic series ($j \in \mathbb{Z}$), we will use the periodicity of this series to reduce the terms on the right side of Eq. (8) and we obtain the following result (see C):

$$\mathbf{M}\ddot{\mathbf{u}} + \mathbf{C}\dot{\mathbf{u}} + \mathbf{K}\mathbf{u} + \mathbf{f}_{NL}(\mathbf{u}, \dot{\mathbf{u}}) = \mathbf{I}_R \left[\sum_{j=-\infty}^{+\infty} \Phi_j P_j \mathrm{e}^{\mathrm{i}\omega_j t} \right] - \left[\sum_{j=-\infty}^{+\infty} F_j^{(1)} \mathrm{e}^{\mathrm{i}\omega_j t} \right] \mathbf{e}_{R_1} - \left[\sum_{j=-\infty}^{+\infty} F_j^{(2)} \mathrm{e}^{\mathrm{i}\omega_j t} \right] \mathbf{e}_{R_2} \tag{11}$$

In the previous equation, we supposed that the solution of the nonlinear problem can admit the same frequencies as the excitation force and the periodical solution of $\mathbf{u}(t)$ which can be represented as shown in the Eq. (30) (see C). $F_j^{(1)}$ and $F_j^{(2)}$ represent the two forces applied on the two rails which are normally different in general.

3 Solution of the problem

In the previous section, the dynamic equation of a railway sleeper has been developed as shown in Eq. (11). We remark that the right side of this equation is the sum of several infinite series. In this section, we present a method to solve this equation with the help of the harmonic balance method and the iterative procedure [47–49] for nonlinear oscillators to develop a numerical method for the dynamic equation of sleepers. Firstly, by using the Fourier development of Eq. (11), we obtain the following result:

$$\frac{1}{T} \int_{-T/2}^{T/2} \left[\mathbf{M}\ddot{\mathbf{u}} + \mathbf{C}\dot{\mathbf{u}} + \mathbf{K}\mathbf{u} + \mathbf{f}_{NL}(\mathbf{u}, \dot{\mathbf{u}})\right] \mathrm{e}^{-\mathrm{i}\omega_j t} \mathrm{d}t = \mathbf{I}_R \Phi_j P_j - \left[F_j^{(1)} \mathbf{e}_{R_1} + F_j^{(2)} \mathbf{e}_{R_2}\right] \tag{12}$$

By inserting Eq. (30) into the last result, this equation can be reduced as follows:

$$-\mathbf{D}_j \Phi_j + \frac{1}{T} \int_{-T/2}^{T/2} \mathbf{f}_{NL}(\mathbf{u}, \dot{\mathbf{u}}) \mathrm{e}^{-\mathrm{i}\omega_j t} \mathrm{d}t = \mathbf{I}_R \Phi_j P_j - \left[F_j^{(1)} \mathbf{e}_{R_1} + F_j^{(2)} \mathbf{e}_{R_2}\right] \tag{13}$$

where $\mathbf{D}_j$ is the dynamic stiffness matrix of the model which is calculated by $\mathbf{D}_j = \omega_j^2 \mathbf{M} - \mathrm{i}\omega_j \mathbf{C} - \mathbf{K}$ and:

$$\begin{cases} \dot{\mathbf{u}}(t) = \displaystyle\sum_{j=-\infty}^{\infty} \mathrm{i}\omega_j \Phi_j \mathrm{e}^{\mathrm{i}\omega_j t} \\ \ddot{\mathbf{u}}(t) = \displaystyle\sum_{j=-\infty}^{\infty} -\omega_j^2 \Phi_j \mathrm{e}^{\mathrm{i}\omega_j t} \end{cases}$$

We remark that Eq. (13) is the harmonic balance form of Eq. (12). The set of this equation for all $j \in \mathbb{Z}$ generates a system of equations with regard to Φ_j which are to be determined.

The railway sleeper is modeled by the finite element method and we note that the index $_L$, $_M$, $_R$, $_{R_1}$ and $_{R_2}$ are respectively the degrees of freedom at the left, middle, right of the sleeper and positions of the forces 1 and 2 (see Fig. 2). In the case of linearity of the foundation, which means that $\mathbf{f}_{NL}(\mathbf{u}, \dot{\mathbf{u}}) = \mathbf{0}$, Eq. (13) can be explained as follows:

$$\begin{bmatrix} \mathbf{D}_{j_{LL}} & \mathbf{D}_{j_{LR_2}} & \mathbf{D}_{j_{LM}} & \mathbf{D}_{j_{LR_1}} & \mathbf{D}_{j_{LR}} \\ \mathbf{D}_{j_{R_2L}} & \tilde{\mathbf{D}}_{j_{R_2R_2}} & \mathbf{D}_{j_{R_2M}} & \mathbf{D}_{j_{R_2R_1}} & \mathbf{D}_{j_{R_2R}} \\ \mathbf{D}_{j_{ML}} & \mathbf{D}_{j_{MR_2}} & \mathbf{D}_{j_{MM}} & \mathbf{D}_{j_{MR_1}} & \mathbf{D}_{j_{MR}} \\ \mathbf{D}_{j_{R_1L}} & \mathbf{D}_{j_{R_1R_2}} & \mathbf{D}_{j_{R_1M}} & \tilde{\mathbf{D}}_{j_{R_1R_1}} & \mathbf{D}_{j_{R_1R}} \\ \mathbf{D}_{j_{RL}} & \mathbf{D}_{j_{RR_2}} & \mathbf{D}_{j_{RM}} & \mathbf{D}_{j_{RR_1}} & \mathbf{D}_{j_{RR}} \end{bmatrix} \begin{bmatrix} \Phi^L_{j_L} \\ \Phi^L_{j_{R_2}} \\ \Phi^L_{j_M} \\ \Phi^L_{j_{R_1}} \\ \Phi^L_{j_R} \end{bmatrix} = \begin{bmatrix} 0 \\ F_j^{(2)} \\ 0 \\ F_j^{(1)} \\ 0 \end{bmatrix} \tag{14}$$

where Φ^L_j is the solution in the case of a linear foundation and:

$$\begin{cases} \tilde{\mathbf{D}}_{j_{R_1R_1}} = \mathbf{D}_{j_{R_1R_1}} + P_j \\ \tilde{\mathbf{D}}_{j_{R_2R_2}} = \mathbf{D}_{j_{R_2R_2}} + P_j \end{cases}$$

The solution of Eq. (14) can be calculated easily for all $j \in \mathbb{Z}$ as follows:

$$\begin{bmatrix} \Phi^L_{j_L} \\ \Phi^L_{j_{R_2}} \\ \Phi^L_{j_M} \\ \Phi^L_{j_{R_1}} \\ \Phi^L_{j_R} \end{bmatrix} = \begin{bmatrix} \mathbf{D}_{j_{LL}} & \mathbf{D}_{j_{LR_2}} & \mathbf{D}_{j_{LM}} & \mathbf{D}_{j_{LR_1}} & \mathbf{D}_{j_{LR}} \\ \mathbf{D}_{j_{R_2L}} & \tilde{\mathbf{D}}_{j_{R_2R_2}} & \mathbf{D}_{j_{R_2M}} & \mathbf{D}_{j_{R_2R_1}} & \mathbf{D}_{j_{R_2R}} \\ \mathbf{D}_{j_{ML}} & \mathbf{D}_{j_{MR_2}} & \mathbf{D}_{j_{MM}} & \mathbf{D}_{j_{MR_1}} & \mathbf{D}_{j_{MR}} \\ \mathbf{D}_{j_{R_1L}} & \mathbf{D}_{j_{R_1R_2}} & \mathbf{D}_{j_{R_1M}} & \tilde{\mathbf{D}}_{j_{R_1R_1}} & \mathbf{D}_{j_{R_1R}} \\ \mathbf{D}_{j_{RL}} & \mathbf{D}_{j_{RR_2}} & \mathbf{D}_{j_{RM}} & \mathbf{D}_{j_{RR_1}} & \mathbf{D}_{j_{RR}} \end{bmatrix}^{-1} \begin{bmatrix} 0 \\ F_j^{(2)} \\ 0 \\ F_j^{(1)} \\ 0 \end{bmatrix} \tag{15}$$

Here now, we denote the right term of Eq. (14) as the vectors $\mathbf{F}_j$. For the non-linear foundation, the term $\mathbf{f}_{NL}(\mathbf{u}, \dot{\mathbf{u}})$ appears and we will use an iteration procedure to solve this problem. Eq. (13) can be rewritten as follows:

$$\mathbf{D}_j \Phi_j = \mathbf{F}_j + \frac{1}{T} \int_{-T/2}^{T/2} \mathbf{f}_{NL}(\mathbf{u}, \dot{\mathbf{u}}) \mathrm{e}^{-\mathrm{i}\omega_j t} \mathrm{d}t \tag{16}$$

The iteration procedure considers the n first harmonics of the periodic solution, thus, the nodal displacement of sleeper can be determined as:

$$\mathbf{u}_{nm}(t) = \sum_{j=-n}^{n} \Phi_j^m \mathrm{e}^{\mathrm{i}\omega_j t} \qquad (\forall m \geq 1) \tag{17}$$

By taking $\Phi_j^1 = \mathbf{0}\ \forall j$, we built a series of vector $\{\Phi_j^m\}$ such that $\Phi_j^m \to \Phi_j$ when $m, n \to \infty$. The index m is understood as the number of the iteration procedures, which can be defined as follows:

$$\mathbf{D}_j \Phi_j^{m+1} = \mathbf{F}_j + \mathbf{Q}_j^m \tag{18}$$

where $\mathbf{Q}_j$ represents a vector of non-linear terms which is calculated by:

$$\mathbf{Q}_j = \frac{1}{T} \int_{-T/2}^{T/2} \mathbf{f}_{NL}(\mathbf{u}, \dot{\mathbf{u}}) \mathrm{e}^{-\mathrm{i}\omega_j t} \mathrm{d}t$$

The series of vectors $\{\Phi_j^m\}$ can be determined from Eq. (18) as follows:

$$\Phi_j^{m+1} = \mathbf{D}_j^{-1} \left(\mathbf{F}_j + \mathbf{Q}_j^m \right) \tag{19}$$

The last equation defines recurrent sequences of the vectors $\{\Phi_j\}$ with regard to m. In the case of convergence of these sequences for all $j \in \mathbb{Z}$ when $m, n \to \infty$, Φ_j^m and Φ_j^{m+1} are replaced by their limit, which we can find once again with Eq. (13). It means that these sequences converge to the solution of this equation. Consequently, the approximation of the periodic solution from Eq. (17) is found by using the sequence of vectors $\{\Phi_j\}$ when m is large enough. In the next section, these sequences will be used to compute the dynamic responses of the railway sleeper.

4 Numerical applications

A numerical model of the sleeper has been created with the help of ABAQUS software by considering a uniform section beam with the cross-section 0.1927 m$\times$ 0.2841 m. The beam length is $2L$ = 2.41m. The track gauge is $2a$ = 1.435m. The mesh of the model is generated with 76 nodes and 75 elements. The element type is 2 node-linear beam element (B21) where each node has 3 DOFs (2 displacements and 1 rotation). This element type corresponds to the Timoshenko beam model. We remark that Tran et al. [46] demonstrated analytically the small difference in sleeper responses (3%) by using the two beam models for the railway sleeper. The material properties of rail pad, sleeper, foundation and parameters of periodic train loads are given in Tab. 1. These parameters will be used for the numerical examples.

4.1 Linear foundation

An analytical model of the railway sleeper posed on a Kelvin-Voigt foundation has been developed by Tran et al. [46]. In this research, the sleeper is modeled with the help of the Timoshenko beam model and its responses are calculated by using the Green's function. When the beam is modeled by FEM, the solutions are given by Eq. (15).

A comparison of sleeper responses of the 2 models is shown in Fig. 4. In this figure, we present a sleeper displacement and sleeper strain at two positions (rail seat and center) of the sleeper in one period of the moving loads, which corresponds to the time where the train moves a distance of a wagon H_w. In this example, the displacement at the rail seat is larger than the one at the

Content	Notation	Value	Unit
Young's modulus of the sleeper	E_s	48	GPa
Shear modulus of the sleeper	G_s	20	GPa
Shear coefficient of the sleeper	κ_s	0.845	
Second moment of the sleeper	I_s	1.694×10^{-4}	m^4
Sleeper density	ρ_s	2658	kgm^{-3}
Stiffness of rail pad	k_{rp}	192	MNm^{-1}
Damping coefficient of rail pad	ζ_{rp}	1.96	MNsm^{-1}
Stiffness of foundation	k_f	440	MNm^{-1}
Damping coefficient of foundation	ζ_f	58.8	kNsm^{-1}
Wagon length	H_w	20	m
Distance of the wagon bogie wheels	D_w	1.8	m
Distance of wagon inner wheels	L_w	8.5	m

Table 1: Materials properties of the rail pad, sleeper and foundation [20]

middle of the sleeper as demonstrated in Fig. 4a. Besides, Fig. 4b shows that the sleeper is in compression at the rail seat (strain negative), while it is in traction at the center (strain positive). The reference time $t = 0$ corresponds

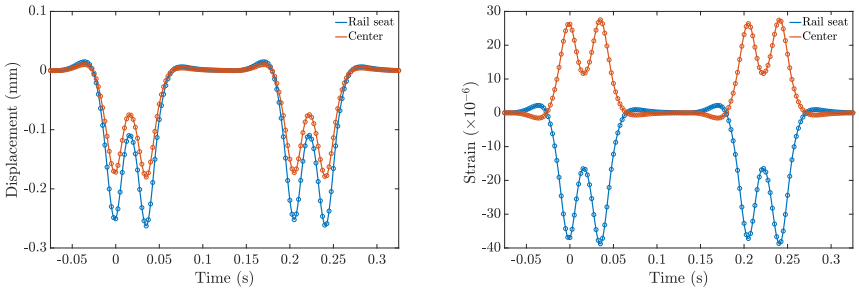

(a) Sleeper displacement

(b) Sleeper strain

Fig. 4: Comparison of the analytical (continuous line) and numerical models (circle)

to the moment when the first wheel passes over the sleeper. In this figure, we can conclude that the two models give the same results, which confirms the validity of the FEM model.

Alternatively, by substituting $\mathbf{f}_{NL}(\mathbf{u}, \dot{\mathbf{u}}) = \mathbf{0}$ into Eq. (18), the non-linear term is avoided: $\mathbf{Q}_j^m = 0$. The solutions of the problem can be calculated by iteration procedures as follows:

$$\Phi_j^{m+1} = \mathbf{D}^{-1}\mathbf{F}_j$$

If the convergence of $\{\Phi_j\}$ is satisfied, the iteration procedure converges to the analytical result. Fig. 5 shows the comparison of the sleeper displacement and sleeper strain when the moving load passes the sleeper at the reference time

($t = 0$). The calculations have been computed with the number of harmonics $n = 25$. The numerical results agree well with the analytical solutions (blue

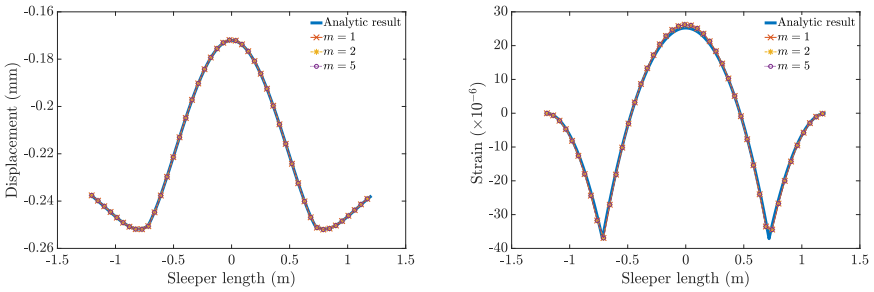

(a) Sleeper displacement (b) Sleeper strain

Fig. 5: Comparison of dynamic responses of sleeper obtained by analytical solution and iteration procedures

line). In this figure, we show the numerical results calculated after 3 iterations: $m = 1, 2, 5$. We see that, in the case of a linear foundation, the convergence of solutions is obtained after 2 iterations.

4.2 Examples of nonlinear foundations

4.2.1 Cubic-nonlinear foundation

In this example, we consider that the nonlinear part of the foundation obeys a cubic law which can be written as follows:

$$\mathbf{f}_{NL_i}(\mathbf{u}_i, \dot{\mathbf{u}}_i) = \varepsilon_c k_c \begin{bmatrix} 0 \\ -\left(u_z\left(x_i\right)\right)^3 \\ 0 \end{bmatrix}$$

The values $\varepsilon_c = 1$ and $k_c = 440 \times 10^7$ MNm^{-3}. Other track parameters are chosen in Tabs. 1 and 2. The numerical results are calculated with a number of harmonics $n = 50$ and $n_0 = 0$. As the sleeper responses are the same when the two bogies pass, the numerical results which are shown in this example correspond to a passage of one bogie. Fig. 6 presents the results for different numbers of iterations m. We note that when $m \geq 4$, the responses are almost unchanged and the convergence of the iteration procedures is satisfied.

Fig. 7 shows the effect of the nonlinear parameter ε_c on the sleeper displacement. We have investigated several different values of ε_c. The foundation is linear when $\varepsilon_c = 0$. The foundation becomes stiffer when this parameter is bigger, thus the amplitude of displacement decreases. This phenomenon is well demonstrated in this figure.

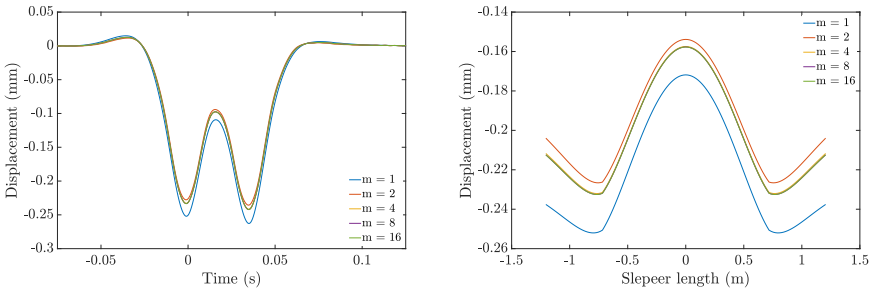

(a) Rail seat (b) Deformed shape

Fig. 6: Numerical results of cubic-nonlinear foundation computed by different number of iterations

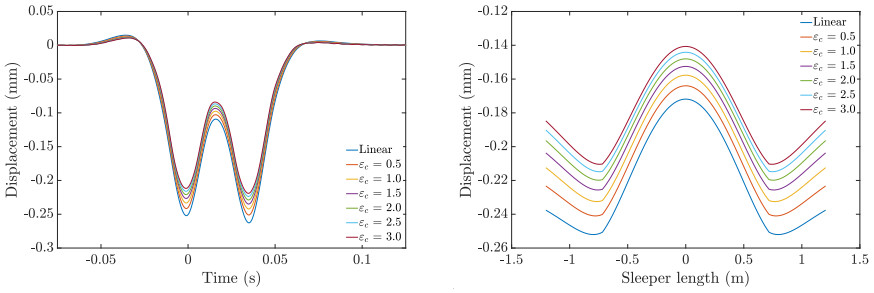

(a) Rail seat (b) Deformed shape

Fig. 7: Effect of the nonlinear parameter of cubic-nonlinear foundation on the sleeper displacements

4.2.2 Bi-linear foundation

Several researches demonstrated that the ballast has different linear behaviors in compression and tension. We consider that the constitutive law of the foundation can be described by a stiffness in compression $\left(k_f^+\right)$ and in tension $\left(k_f^-\right)$. In addition, the damping coefficient of the foundation (ζ_f) is considered as unchanged in the two cases. Due to the separation of the linear and nonlinear parts in the model, the nonlinear term can be rewritten as follows:

$$\mathbf{f}_{NL}(\mathbf{u}, \dot{\mathbf{u}}) = \begin{cases} \left(k_f^+ - k_f\right) u_p & \text{if} \quad u_p < 0 \\ \left(k_f^- - k_f\right) u_p & \text{if} \quad u_p \geq 0 \end{cases}$$

where u_p presents a component p of the vector displacement $\mathbf{u}$ with $(p \in [1, 3n_n])$. In this example, the sleeper displacements are calculated with the two stiffness of foundation: $k_f^+ = 440$ MNm^{-1} and $k_f^- = 352$ MNm^{-1}. Fig. 8

shows the numerical results computed by different number of iterations while the number of harmonics is $n = 25$. The iteration procedures converges when the number is bigger than 8. Fig. 8b shows that the deformed shape of the sleeper at the reference time is almost unchanged when $m \geq 8$.

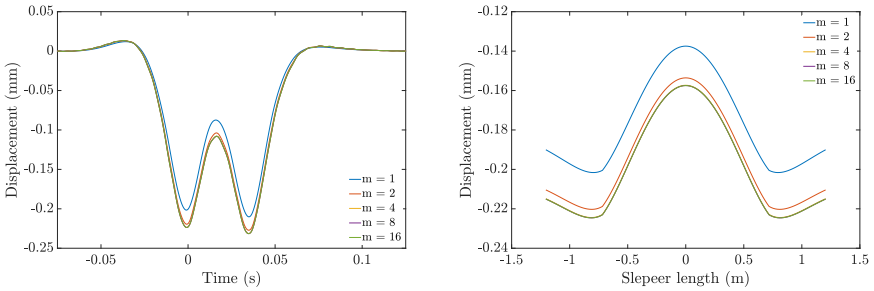

(a) Rail seat (b) Deformed shape

Fig. 8: Numerical results of bi-linear foundation computed by different number of iterations

Next, the influence of the number of harmonics on the sleeper responses is shown in Fig. 9. When $n \geq 8$, we find that the solution has converged. Consequently, this study demonstrates that the lower harmonics are more important than the higher. Put differently, the higher order harmonics can be neglected in this case.

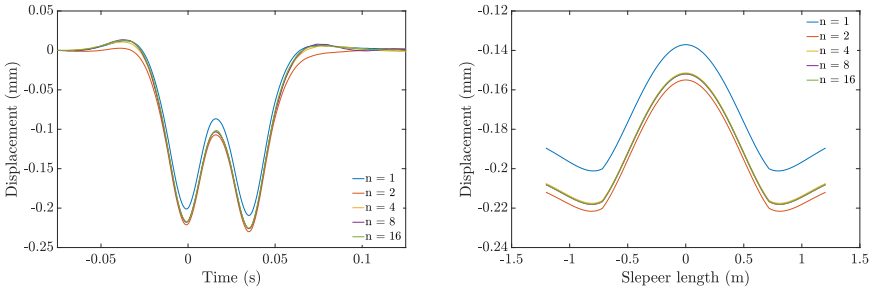

(a) Rail seat (b) Deformed shape

Fig. 9: Numerical results of bi-linear foundation computed by different number of harmonics

Finally, the effect of the nonlinear parameter $r = k_f^-/k_f^+$ on the sleeper displacement is shown in Fig. 10. This ratio is calculated by changing the stiffness k_f^- while maintaining k_f^+ as constant. For each r value, the track

responses have been calculated with the same numbers of iterations, but the convergence of solutions is always satisfied. The deformed shape is obtained at the reference time: $t = 0$, when the first wheel moves over the sleeper. This parameter indicates a foundation with equal stiffness in compression and tension when $r = 1$, and a foundation that cannot support any tension when $r = 0$. We see that the sleeper displacements are greater when the foundation has a smaller tension stiffness.

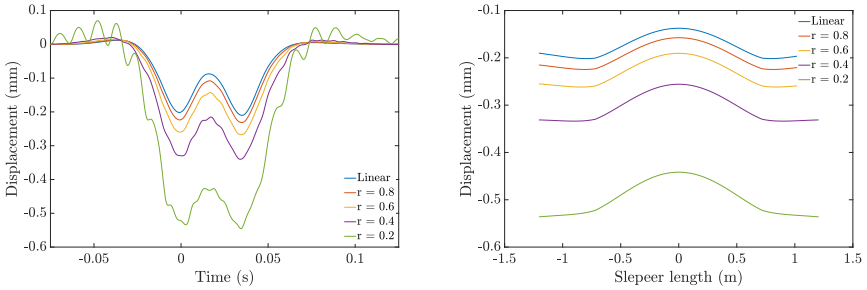

(a) Rail seat (b) Deformed shape

Fig. 10: Effect of the nonlinear parameter of the bi-linear foundation on the sleeper displacements

4.2.3 Influence of the nonlinear parameters on the sleeper strain

Here, we study the influence of the nonlinear parameter on the sleeper strain. In Fig. 11, we plot the sleeper strain at the rail seat in function of the sleeper at

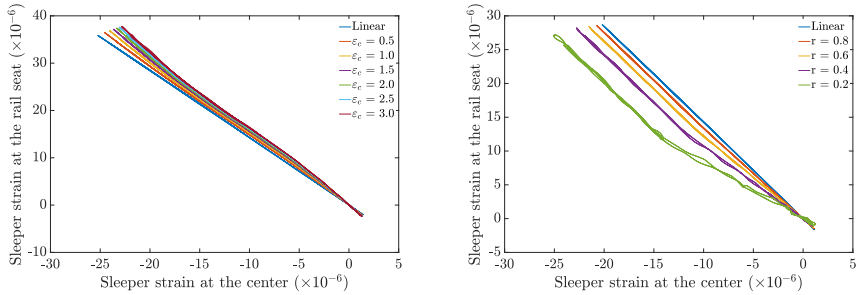

(a) Cubic-nonlinear foundation (b) Bi-linear foundation

Fig. 11: Influence of the nonlinear parameters on the sleeper strain

the center of the sleeper in one period of moving loads. In the linear case, this

ratio is related by a linear relation (blue lines in the Figs. 11a and 11b). When the nonlinear term of the foundation obeys a cubic law, the sleeper strain at the center is more important than the ones at the rail seat. In the bi-linear case, the relationship between the sleeper strain at the two positions which are shown in Fig. 11 presents clearly two linear behaviors of the foundations.

5 Conclusions

In this paper, the dynamics response of a railway track posed on a nonlinear foundation has been studied by a semi-analytical model. The iteration method has been developed which permits to obtain fast results. The convergence of the method is also studied with numerical examples (linear and non-linear). Thus, the dynamic responses of the nonlinear track can be calculated quickly. In addition, this model can be applicable for different nonlinear foundations. The numerical examples shows that the ratio between the strain at rail seats and center of the sleeper depends on the foundation behavior. This result is significant and can be used to study the foundation in the future work.

Acknowledgements Tran Le Hung, ID VNU.2021.TTS14, thanks The Development Foundation of Vietnam National University, Hanoi for sponsoring this research.

Conflict of interest

The author(s) declared no potential conflicts of interest with respect to the research, authorship, and/or publication of this article.

Funding

The author(s) received no financial support for the research, authorship, and/or publication of this article.

Data availability statements

Data sharing not applicable to this article as no datasets were generated or analyzed during the current study.

A Mathematical transformation

By performing the Fourier transform, and then the inverse Fourier transform of the right term of the Eq. (7), we can obtain the following result:

$$k_{rp}w_r(t) + \zeta_{rp}\dot{w}_r(t) = \frac{1}{2\pi}\int_{-\infty}^{+\infty} k_p\hat{w}_r(\omega)\mathrm{e}^{\mathrm{i}\omega t}\mathrm{d}\omega \tag{20}$$

The right term of the last equation depends on the rail displacements. It can be rewritten as a function of the sleeper displacement by substituting Eq. (6) into Eq. (20) as follows:

$$\frac{1}{2\pi}\int_{-\infty}^{+\infty} k_p \hat{w}_r(\omega)\mathrm{e}^{\mathrm{i}\omega t}\mathrm{d}\omega = \frac{1}{2\pi}\int_{-\infty}^{+\infty} \frac{k_p^2 \hat{u}_{R_{kz}}(\omega)}{k_p + \mathcal{K}_e}\mathrm{e}^{\mathrm{i}\omega t}\mathrm{d}\omega - \frac{1}{2\pi}\int_{-\infty}^{+\infty} \frac{k_p \mathcal{Q}_e}{k_p + \mathcal{K}_e}\mathrm{e}^{\mathrm{i}\omega t}\mathrm{d}\omega$$

By combining the previous result and Eq. (7), we obtain the following result:

$$\begin{aligned}\mathbf{M}\ddot{\mathbf{u}} + \mathbf{C}\dot{\mathbf{u}} + \mathbf{K}\mathbf{u} + \mathbf{f}_{NL}(\mathbf{u},\dot{\mathbf{u}}) = &\left[\frac{1}{2\pi}\int_{-\infty}^{+\infty} \frac{k_p^2 \hat{u}_{R_{1z}}(\omega)}{k_p + \mathcal{K}_e}\mathrm{e}^{\mathrm{i}\omega t}\mathrm{d}\omega\right]\mathbf{e}_{R_1} \\ &- \left[\frac{1}{2\pi}\int_{-\infty}^{+\infty} \frac{k_p \mathcal{Q}_1(\omega)}{k_p + \mathcal{K}_e}\mathrm{e}^{\mathrm{i}\omega t}\mathrm{d}\omega\right]\mathbf{e}_{R_1} \\ &+ \left[\frac{1}{2\pi}\int_{-\infty}^{+\infty} \frac{k_p^2 \hat{u}_{R_{2z}}(\omega)}{k_p + \mathcal{K}_e}\mathrm{e}^{\mathrm{i}\omega t}\mathrm{d}\omega\right]\mathbf{e}_{R_2} \\ &- \left[\frac{1}{2\pi}\int_{-\infty}^{+\infty} \frac{k_p \mathcal{Q}_2(\omega)}{k_p + \mathcal{K}_e}\mathrm{e}^{\mathrm{i}\omega t}\mathrm{d}\omega\right]\mathbf{e}_{R_2}\end{aligned} \tag{21}$$

where $\mathcal{Q}_1(\omega)$ and $\mathcal{Q}_2(\omega)$ are the equivalent train loads at the rail 1 and rail 2 respectively (see Appendix B). $\hat{u}_{R_{1_z}}$ and $\hat{u}_{R_{2_z}}$ are respectively the two displacement of the sleeper at the crossing points with the two rails in the frequency domain. By developing the first and the third terms on the right side of Eq. (8), it can be rewritten as follows:

$$\begin{cases}\left[\frac{1}{2\pi}\int_{-\infty}^{+\infty} \frac{k_p^2 \hat{u}_{R_{1z}}(\omega)}{k_p + \mathcal{K}_e}\mathrm{e}^{\mathrm{i}\omega t}\mathrm{d}\omega\right]\mathbf{e}_{R_1} = \mathbf{I}_{R_1}\left[\frac{1}{2\pi}\int_{-\infty}^{+\infty} \frac{k_p^2 \hat{\mathbf{u}}(\omega)}{k_p + \mathcal{K}_e}\mathrm{e}^{\mathrm{i}\omega t}\mathrm{d}\omega\right] \\ \left[\frac{1}{2\pi}\int_{-\infty}^{+\infty} \frac{k_p^2 \hat{u}_{R_{2z}}(\omega)}{k_p + \mathcal{K}_e}\mathrm{e}^{\mathrm{i}\omega t}\mathrm{d}\omega\right]\mathbf{e}_{R_2} = \mathbf{I}_{R_2}\left[\frac{1}{2\pi}\int_{-\infty}^{+\infty} \frac{k_p^2 \hat{\mathbf{u}}(\omega)}{k_p + \mathcal{K}_e}\mathrm{e}^{\mathrm{i}\omega t}\mathrm{d}\omega\right]\end{cases}$$

Finally, by inserting the last result in Eq. (21), we have:

$$\begin{aligned}\mathbf{M}\ddot{\mathbf{u}} + \mathbf{C}\dot{\mathbf{u}} + \mathbf{K}\mathbf{u} + \mathbf{f}_{NL}(\mathbf{u},\dot{\mathbf{u}}) = &\mathbf{I}_R\left[\frac{1}{2\pi}\int_{-\infty}^{+\infty} \frac{k_p^2 \hat{\mathbf{u}}(\omega)}{k_p + \mathcal{K}_e}\mathrm{e}^{\mathrm{i}\omega t}\mathrm{d}\omega\right] \\ &- \left[\frac{1}{2\pi}\int_{-\infty}^{+\infty} \frac{k_p \mathcal{Q}_1(\omega)}{k_p + \mathcal{K}_e}\mathrm{e}^{\mathrm{i}\omega t}\mathrm{d}\omega\right]\mathbf{e}_{R_1} \\ &- \left[\frac{1}{2\pi}\int_{-\infty}^{+\infty} \frac{k_p \mathcal{Q}_2(\omega)}{k_p + \mathcal{K}_e}\mathrm{e}^{\mathrm{i}\omega t}\mathrm{d}\omega\right]\mathbf{e}_{R_2}\end{aligned} \tag{22}$$

B Periodically supported beam in steady-state

Fig. 12 presents a periodically supported beam model. In this model, each rail k of the track is modeled by an infinite beam posed on periodic supports. The sleeper spacing is l. The train loads are considered by the concentrated loads $Q_j^{(k)}$. Each load is characterized by its distance D_j to the first axle and the train speed v.

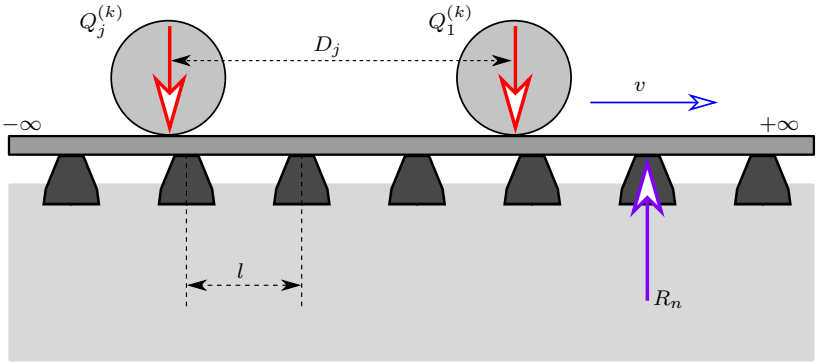

Fig. 12: Periodically supported beam model

In the frequency domain, Hoang et al. [42,43] have demonstrated a relation between the reaction force $\hat{R}_k(\omega)$ and the displacement of the rail $\hat{w}_r(0,\omega)$ in the frequency domain as follows:

$$\hat{R}_k(\omega) = \mathcal{K}_e \hat{w}_r(0,\omega) + \mathcal{Q}_k \tag{23}$$

where: $\mathcal{K}_e$ and $\mathcal{Q}_k$ are the equivalent stiffness and equivalent loads of the system. The two functions are calculated by the parameters of the rail and the train loads as follows:

$$\begin{cases} \mathcal{K}_e(\omega) = 4\lambda_r^3 E_r I_r \left[\dfrac{\sin l\lambda_r}{\cos l\lambda_r - \cos\frac{\omega l}{v}} - \dfrac{\sinh l\lambda_r}{\cosh l\lambda_r - \cos\frac{\omega l}{v}} \right]^{-1} \\ \mathcal{Q}_k(\omega) = \dfrac{\mathcal{K}_e(\omega)}{v E_r I_r \left[\left(\frac{\omega}{v}\right)^4 - \lambda_r^4 \right]} \sum_{j=1}^{K} Q_j^{(k)} \mathrm{e}^{-\mathrm{i}\omega\frac{D_j}{v}} \end{cases} \tag{24}$$

where: $\lambda_r = \sqrt[4]{\dfrac{\rho_r S_r \omega^2}{E_r I_r}}$. E_r, I_r, ρ_r and S_r are respectively the Young's modulus of rail, the second moment of area of the rail, the density of rail and cross-sectional area of rail. The expressions show that Eq. (23) is applicable for any foundation behavior. In this paper, the rail parameters are given in Tab. 2.

Content	Notation	Value	Unit
Young's modulus of the rail	E_r	210	GPa
Second moment of area of the rail	I_r	$3{\times}10^{-5}$	m^4
Rail density	ρ_r	7850	kgm^{-3}
Rail cross-sectional area	S_r	7.69×10^{-3}	m^2
Sleeper spacing	l	0.6	m
Moving force rail 1	Q_1	80	kN
Moving force rail 2	Q_2	80	kN
Train speed	v	50	ms^{-1}

Table 2: Parameters of the periodically supported beam model [42]

C Calculation of equivalent load

By substituting Eq. (9) into Eq. (24) and together with the assumption (10), a new expression of the equivalent charge $\mathcal{Q}_k(\omega)$ can be expressed as follows:

$$\mathcal{Q}_k = \frac{Q\mathcal{K}_e}{vE_rI_r} \frac{\left(1+\mathrm{e}^{-\mathrm{i}\omega\frac{D_w}{v}}+\mathrm{e}^{-\mathrm{i}\omega\frac{D_w+L_w}{v}}+\mathrm{e}^{-\mathrm{i}\omega\frac{2D_w+L_w}{v}}\right)}{\left(\frac{\omega}{v}\right)^4-\lambda_r^4} \sum_{j=-\infty}^{\infty} \mathrm{e}^{-\mathrm{i}\omega\frac{H_w}{v}j} \tag{25}$$

The parameters of Eq. (25) are explained in B. Moreover, a property of the Dirac comb [52] gives the following result:

$$\sum_{j=-\infty}^{\infty} \mathrm{e}^{-\mathrm{i}\omega\frac{H_w}{v}j} = 2\pi\frac{v}{H_w}\sum_{j=-\infty}^{\infty}\delta\left(\omega+\frac{2\pi v}{H_w}j\right) \tag{26}$$

By introducing this property into Eq. (25), the equivalent loads can be expressed as follows:

$$\mathcal{Q}_k = \frac{2\pi Q\mathcal{K}_e}{E_rI_rH_w} \frac{\left(1+\mathrm{e}^{-\mathrm{i}\omega\frac{D_w}{v}}+\mathrm{e}^{-\mathrm{i}\omega\frac{D_w+L_w}{v}}+\mathrm{e}^{-\mathrm{i}\omega\frac{2D_w+L_w}{v}}\right)}{\left(\frac{\omega}{v}\right)^4-\lambda_r^4} \sum_{j=-\infty}^{\infty}\delta\left(\omega+\frac{2\pi v}{H_w}j\right) \tag{27}$$

Thus, Eq. (27) leads to the following result:

$$\frac{1}{2\pi}\int_{-\infty}^{+\infty}\frac{k_p\mathcal{Q}_k}{k_p+\mathcal{K}_e}\mathrm{e}^{\mathrm{i}\omega t}\mathrm{d}\omega = \sum_{j=-\infty}^{\infty}F_j\mathrm{e}^{\mathrm{i}\omega_j t} \tag{28}$$

where F_j is calculated by:

$$F_j = \frac{Q}{E_rI_rH_w}\left[\frac{1+\mathrm{e}^{-\mathrm{i}\omega\frac{D_w}{v}}+\mathrm{e}^{-\mathrm{i}\omega\frac{D_w+L_w}{v}}+\mathrm{e}^{-\mathrm{i}\omega\frac{2D_w+L_w}{v}}}{\left(\frac{\omega}{v}\right)^4-\lambda_r^4}\frac{k_p\mathcal{K}_e}{k_p+\mathcal{K}_e}\right]_{\omega=\omega_j} \tag{29}$$

The last equation describes a forced oscillation with the exciting force $\sum F_j\mathrm{e}^{\mathrm{i}\omega_j t}$ with frequency $f_0 = v/H_w$. We remark that $\omega_j = 2\pi f_j = 2\pi j f_0$. We suppose that the solution of the nonlinear problem can admit the same frequencies as the excitation force. Therefore, with this assumption, there exists a periodic solution of $\mathbf{u}(t)$ which can be represented as follows:

$$\mathbf{u}(t) = \sum_{j=-\infty}^{\infty}\Phi_j\mathrm{e}^{\mathrm{i}\omega_j t} \tag{30}$$

Moreover, by performing the Fourier transform, Eq. (30) can be explained in the frequency domain as follows:

$$\hat{\mathbf{u}}(\omega) = 2\pi\sum_{j=-\infty}^{\infty}\Phi_j\delta(\omega-\omega_j) \tag{31}$$

So that, we can deduce the following result:

$$\frac{1}{2\pi}\int_{-\infty}^{+\infty}\frac{k_p^2\hat{\mathbf{u}}}{k_p+\mathcal{K}_e}\mathrm{e}^{\mathrm{i}\omega t}\mathrm{d}\omega = \sum_{j=-\infty}^{\infty}\Phi_jP_j\mathrm{e}^{\mathrm{i}\omega_j t} \tag{32}$$

where P_j is calculated by:

$$P_j = \left[\frac{k_p^2}{k_p+\mathcal{K}_e}\right]_{\omega=\omega_j} \tag{33}$$

When $\omega_j = 0$, we have particularly the values: $P_0 = k_{rp}$ and $F_0^{(k)} = 2Q^{(k)}\dfrac{L_w}{H_w}$. Finally, by combining Eqs. (8), (28) and (32), the dynamic equation of the sleeper can be written by:

$$\begin{aligned}\mathbf{M}\ddot{\mathbf{u}} + \mathbf{C}\dot{\mathbf{u}} + \mathbf{K}\mathbf{u} + \mathbf{f}_{NL}(\mathbf{u}, \dot{\mathbf{u}}) = \mathbf{I}_R \left[\sum_{j=-\infty}^{+\infty} \Phi_j P_j \mathrm{e}^{\mathrm{i}\omega_j t}\right] - \left[\sum_{j=-\infty}^{+\infty} F_j^{(1)} \mathrm{e}^{\mathrm{i}\omega_j t}\right] \mathbf{e}_{R_1} \\ - \left[\sum_{j=-\infty}^{+\infty} F_j^{(2)} \mathrm{e}^{\mathrm{i}\omega_j t}\right] \mathbf{e}_{R_2}\end{aligned} \tag{34}$$

References

1. A. Kriloff. Uber die erzwungenen schwingungen von gleichformigen elastischen staben. *Math. Ann.*, 61:211 – 234, 1905.
2. S. Timoshenko. Erzwungene schwingungen prismatischer stäbe. *Z. Math. Phys.*, 59(2):162 – 203, 1905.
3. Ladislav Fryba. *Vibration of solids and structures under moving loads*. Noordhoff International Publishing, 1972.
4. S. Timoshenko, D. Young, and W. Weaver. *Vibration Problems in Engineering*. Wiley, 1974.
5. T.M. Wang and J.E. Stephens. Natural frequencies of Timoshenko beams on pasternak foundations. *Journal of Sound and Vibration*, 51(2):149–155, mar 1977.
6. G.G Adams. Critical speeds and the response of a tensioned beam on an elastic foundation to repetitive moving loads. *International Journal of Mechanical Sciences*, 37(7):773 – 781, 1995.
7. L. Sun. A closed-form solution of a bernoulli-euler beam on a viscoelastic foundation under harmonic line loads. *Journal of Sound and Vibration*, 242(4):619 – 627, 2001.
8. Yung-Hsiang Chen and Yen-Hui Huang. Dynamic characteristics of infinite and finite railways to moving loads. *Journal of Engineering Mechanics*, 129(9):987–995, 2003.
9. A.K. Mallik, Sarvesh Chandra, and Avinash B. Singh. Steady-state response of an elastically supported infinite beam to a moving load. *Journal of Sound and Vibration*, 291(3):1148 – 1169, 2006.
10. Faruk Firat Çalim. Dynamic analysis of beams on viscoelastic foundation. *European Journal of Mechanics - A/Solids*, 28(3):469–476, May 2009.
11. José N. Varandas, Paul Hölscher, and Manuel a.G. Silva. Dynamic behaviour of railway tracks on transitions zones. *Computers & Structures*, 89(13-14):1468–1479, jul 2011.
12. M. Ichikawa, Y. Miyakawa, and A. Matsuda. Vibration analysis of the continuous beam subjected to a moving mass. *Journal of Sound and Vibration*, 230(3):493–506, 2000.
13. D. J. Mead. Wave propagation in continuous periodic structures: research contributions from southampton. *Journal of Sound and Vibration*, 190(3):495–524, 1996.
14. D. J. Mead. Free wave propagation in periodically supported, infinite beams. *Journal of Sound and Vibration*, 11(2):181–197, 1970.
15. A. V. Metrikine and K. Popp. Vibration of a periodically supported beam on an elastic half-space. *European Journal of Mechanics A/Solid*, 18:679–701, 1999.
16. A. V. Vostroukhov and A.V. Metrikine. Periodically supported beam on a visco-elastic layer as a model for dynamic analysis of a high-speed railway track. *International Journal of Solids and Structures*, 40:5723–5752, 2003.
17. P. M. Belotserkovskiy. On the oscillation of infinite periodic beams subjected to a moving concentrated force. *Journal of Sound and Vibration*, 193(3):705–712, 1996.
18. L.-H. Tran, T. Hoang, G. Foret, and D. Duhamel. Calculation of the dynamic responses of a railway track on a non-uniform foundation. *Journal of Vibration and Control*, 523:116730, apr 2022.
19. L.-H. Tran, T. Hoang, F. Gilles, D. Duhamel, S. Messad, and A. Loaëc. Analytical model of the dynamics of railway sleeper. In *6th International Conference on Computational Methods in Structural Dynamics and Earthquake Engineering Methods in Structural Dynamics and Earthquake Engineering*, pages 3937–3948, Rhodes, Greece, 2017.

20. L.-H. Tran, T. Hoang, F. Gilles, D. Duhamel, S. Messad, and A. Loaëc. A fast analytic method to calculate the dynamic response of railways sleepers. *Journal of Vibration and Acoustics*, 141(1), 2019.
21. L.-H. Tran, T. Hoang, D. Duhamel, G. Foret, S. Messad, and A. Loaëc. Influence of non-homogeneous foundations on the dynamic responses of railway sleepers. *International Journal of Structural Stability and Dynamics*, 21(01):2150002, 2021.
22. Hu Ding, Li-Qun Chen, and Shao-Pu Yang. Convergence of Galerkin truncation for dynamic response of finite beams on nonlinear foundations under a moving load. *Journal of Sound and Vibration*, 331(10):2426–2442, May 2012.
23. Hu Ding, Kang Li Shi, Li Qun Chen, and Shao Pu Yang. Dynamic response of an infinite Timoshenko beam on a nonlinear viscoelastic foundation to a moving load. *Nonlinear Dynamics*, 73(1-2):285–298, 2013.
24. S.M. Abdelghany, K.M. Ewis, A.A. Mahmoud, and M.M. Nassar. Dynamic response of non-uniform beam subjected to moving load and resting on non-linear viscoelastic foundation. *Beni-Suef University Journal of Basic and Applied Sciences*, 4(3):192 – 199, 2015.
25. M.H. Kargarnovin, D. Younesian, D.J. Thompson, and C.J.C. Jones. Response of beams on nonlinear viscoelastic foundations to harmonic moving loads. *Computers & Structures*, 83(23-24):1865–1877, September 2005.
26. M. Ansari, E. Esmailzadeh, and D. Younesian. Frequency analysis of finite beams on nonlinear Kelvin–Voight foundation under moving loads. *Journal of Sound and Vibration*, 330(7):1455–1471, March 2011.
27. Hong Yan Chen, Hu Ding, Shao Hua Li, and Li Qun Chen. Convergent term of the Galerkin truncation for dynamic response of sandwich beams on nonlinear foundations. *Journal of Sound and Vibration*, 483:115514, sep 2020.
28. Hong Yan Chen, Hu Ding, Shao Hua Li, and Li Qun Chen. The Scheme to determine the convergence term of the Galerkin method for dynamic analysis of sandwich plates on nonlinear foundations. *Acta Mecanica Solida Sinica*, 34(1):1–11, feb 2021.
29. Anas Ouzizi, Farah Abdoun, and Lahcen Azrar. Nonlinear dynamics of beams on nonlinear fractional viscoelastic foundation subjected to moving load with variable speed. *Journal of Sound and Vibration*, 523:116730, apr 2022.
30. Vu-Hieu Nguyen and Denis Duhamel. Finite element procedures for nonlinear structures in moving coordinates. Part 1: Infinite bar under moving axial loads. *Computers & Structures*, 84(21):1368–1380, 2006.
31. V. H. Nguyen and Denis Duhamel. Finite element procedures for nonlinear structures in moving coordinates. part ii: Infinite beam under moving harmonic loads. *Computers and Structures*, 86:2056–2063, 2008.
32. P. Castro Jorge, F.M.F Simoes, and A. Pinto da Costa. Finite element dynamics analysis of beams on non-uniform nonlinear viscoelastic foundations under moving loads. *Proceeding of the 9th Intenational Conference on Structural Dynamics, EURODYN2014*, 2014.
33. Jen-San Chen and Yung-Kan Chen. Steady state and stability of a beam on a damped tensionless foundation under a moving load. *International Journal of Non-Linear Mechanics*, 46(1):180–185, January 2011.
34. E.J. Sapountzakis and A.E. Kampitsis. Nonlinear response of shear deformable beams on tensionless nonlinear viscoelastic foundation under moving loads. *Journal of Sound and Vibration*, 330(22):5410–5426, October 2011.
35. Xinwen Yang, Yao Shu, and Shunhua Zhou. An explicit periodic nonlinear model for evaluating dynamic response of damaged slab track involving material nonlinearity of damage in high speed railway. *Construction and Building Materials*, 168:606–621, apr 2018.
36. F.S. Samani, F. Pellicano, and A. Masoumi. Performances of dynamic vibration absorbers for beams subjected to moving loads. *Nonlinear Dynamics*, 72:211 – 234, 2013.
37. 0.R. Barry, D.C.D. Oguamanam, and J.W. Zu. Nonlinear vibration of an axially loaded beam carrying multiple mass-spring-damper system. *Nonlinear Dynamics*, 77:1597–1608, 2014.
38. M.A. Bukhari and O.R. Barry. Nonlinear vibrations analysis of overhead power lines: a beam with mass-spring-damper-mass systems. *Journal of Vibration and Acoustics*, 140:260–275, 2017.

39. T. Hoang, D. Duhamel, G. Foret, H.-P. Yin, and G. Cumunel. Response of a periodically supported beam on a nonlinear foundation subjected to moving loads. *Nonlinear Dynamics*, 86(2):953–961, 2016.
40. L.-H. Tran, D.-D. Nguyen. Calculation of the dynamic responses of rails subjected to moving loads on ballasted railway track. *VNU Journal of Science: Mathematics - Physics*, 38(3), 2022.
41. L.-H. Tran, K. Le-Nguyen. Calculation of dynamic responses of a cracked beam on visco-elastic foundation subjected to moving loads, and its application to a railway track model. *International Journal of Applied Mechanics*, 15(2), 2023.
42. T. Hoang, D. Duhamel, G. Foret, H.P. Yin, P. Joyez, and R. Caby. Calculation of force distribution for a periodically supported beam subjected to moving loads. *Journal of Sound and Vibration*, 388:327 – 338, 2017.
43. T. Hoang, D. Duhamel, and G. Foret. Dynamical response of a timoshenko beams on periodical nonlinear supports subjected to moving forces. *Engineering Structures*, 176:673 – 680, 2018.
44. Ali H. Nayfeh. *Introduction to perturbation techniques*. Wiley Classics Library Edition, 1993.
45. Ali H. Nayfeh and Dean T. Mook. *Nonlinear oscillations*. Wiley Classics Library Edition, 1995.
46. L.-H. Tran, K. Le-Nguyen, and T. Hoang. A comparison of beam models for the dynamics of railway sleepers. *International Journal of Rail Transportation*, 10(2), 2022.
47. R.E. Mickens. A generalization of the method of harmonic balance. *Journal of Sound and Vibration*, 111(3):515 – 518, 1986.
48. Ronald E. Mickens. A generalized iteration procedure for calculating approximations to periodic solutions of truly nonlinear oscillators. *Journal of Sound and Vibration*, 287(4):1045 – 1051, 2005.
49. T. Hoang, D. Duhamel, G. Foret, H.P. Yin, and P. Argoul. Frequency dependent iteration method for forced nonlinear oscillators. *Applied Mathematical Modelling*, 42:441 – 448, 2017.
50. L.-H. Tran. *Developpement de traverses instrumentées pour l'étude du comportement des voies ferrées*. PhD thesis, ENPC, Paris-Est, 2020.
51. T. S. Azoh, W. Nzie, B. Djeumako, and B. S. Fotsing. Modeling of train track vibrations for maintenance perspectives: application. *European Scientific Journal*, 10(21):260–275, 2014.
52. R.N. Bracewell. *The Fourier transform and its applications*. McGraw-Hill Higher Education, 2000.